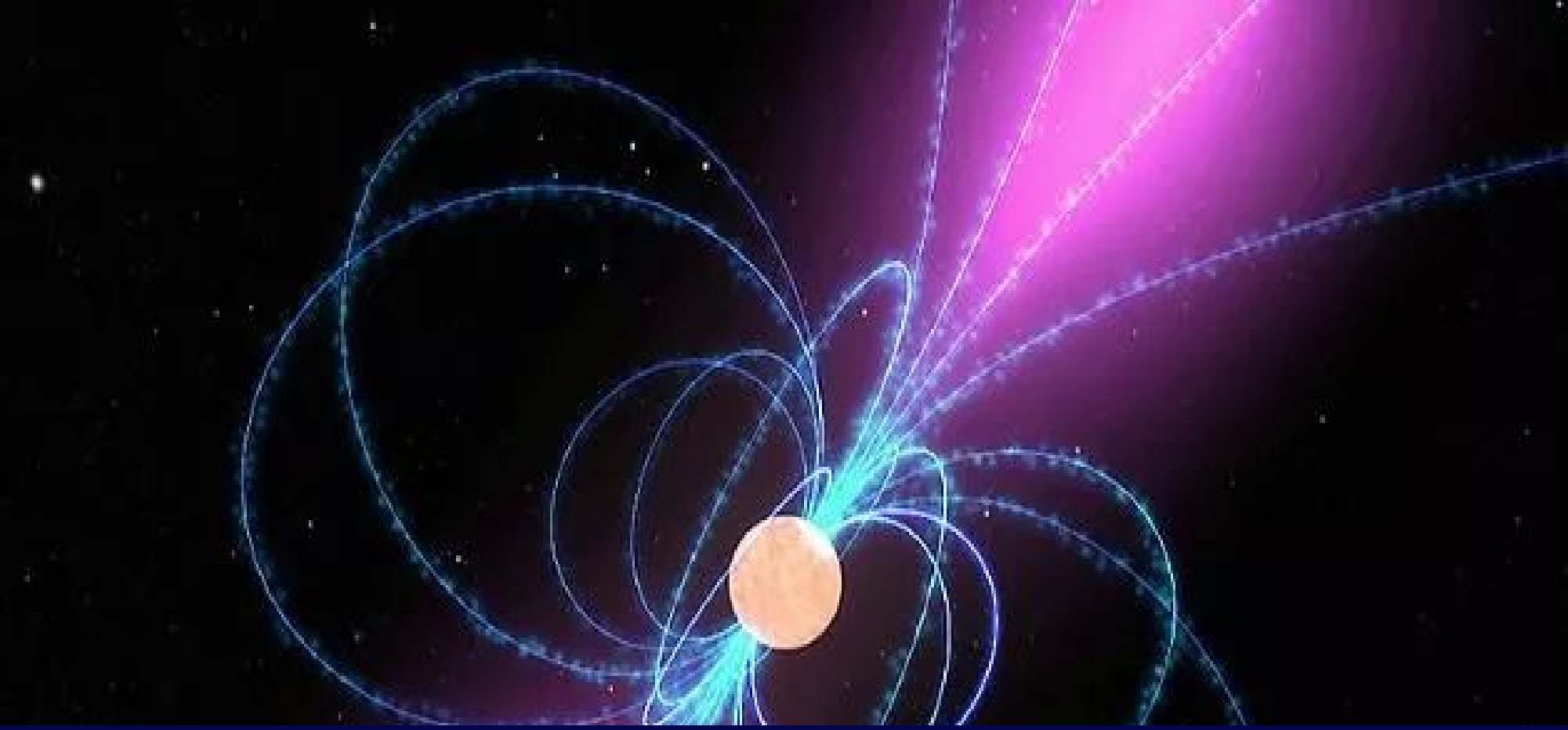

Universal Relations in the Emergence of Special Points on Mass-Radius Relation of Hybrid Stars

Debashree Sen
Center for Extreme Nuclear Matters (CENuM), Korea University
Collaborators: N. Alam & G. Chaudhuri, VECC, Kolkata, India

(14th APCTP-BLTP JINR Joint Workshop, Posco International Center (PIC), Pohang)

Table of Contents

Neutron Stars and Pulsar Observations

Neutron Stars (NSs) are remnants of massive stars after thermo-nuclear runaway. They are mostly observed as pulsars with particular and very accurate rotational period and emission of electromagnetic waves.

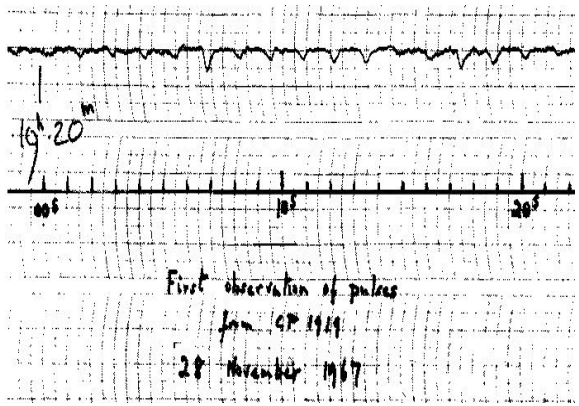

Present Day Astrophysical Constraints

Maximum mass (PSR J0740+6620) : $M = 2.08 \pm 0.07\ M_\odot$

Corresponding radius : $R = 13.7^{+2.6}_{-1.5}$ km

$R = 12.39^{+1.30}_{-0.98}$ km

Radius of $1.4M_\odot$ NS (GW170817) : $8.9 \leq R_{1.4} \leq 13.2$ km

Tidal deformability of $1.4M_\odot$ NS : $70 \leq \Lambda_{1.4} \leq 580$

NICER (PSR J0030+0451) : $M = 1.34^{+0.15}_{-0.16}\ M_\odot$; $R = 12.71^{+1.14}_{-1.19}$ km

$M = 1.44^{+0.15}_{-0.14}\ M_\odot$; $R = 13.02^{+1.24}_{-1.06}$ km

Characteristics

Density : $\rho \approx (5-10)\rho_0$
Compactness : M/R $\approx$ 0.2 and
Temperature : a few Kelvin $\approx$ 0 MeV (negligible)

Experiments till date have examined nuclear matter at saturation density $\rho_0 = 0.16 fm^{-3}$ and upto $\approx$4.5ρ_0. So, the composition, equation of state (EoS) and structure of NSs are determined by the theoretical modeling of NS matter (NSM).

Possible Composition

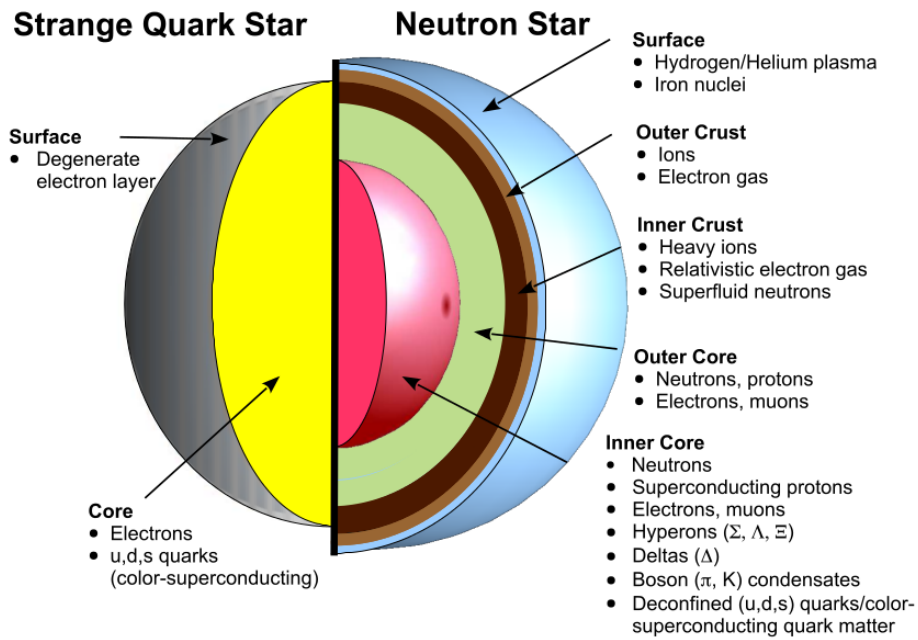

Crust: thickness upto 1 km and density upto $\rho > 10^7$ gm cm^{-3}. It is described with the BPS EoS [1] including the pasta phases [2]

Outer core: Density : $\rho \sim 10^{14}$ gm cm^{-3}
β stable NSM (n,p,e,μ)

Inner core: Density : $\rho > 10^{14}$ gm cm^{-3}
Exotic forms of matter : Hyperons, Δ baryons, boson condensates
Deconfined quark matter

[1] G. Baym, C. Pethick, and P. Sutherland, APJ 170, 299 (1971)
[2] F. Grill et al., Phys. Rev. C 90, 045803 (2014)

Hadron-Quark Phase Transition

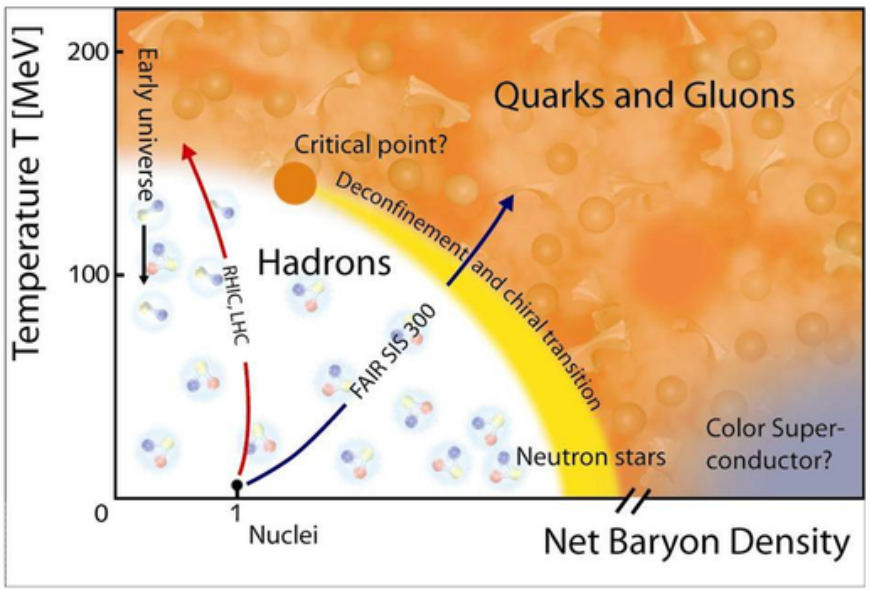

QCD Phase Diagram

nature physics
LETTERS
https://doi.org/10.1038/s41567-020-0914-9
Check for updates

OPEN

Evidence for quark-matter cores in massive neutron stars

Eemeli Annala[1], Tyler Gorda[2], Aleksi Kurkela[3,4], Joonas Nättilä[5,6,7] and Aleksi Vuorinen[1]

The theory governing the strong nuclear force—quantum chromodynamics—predicts that at sufficiently high energy densities, hadronic nuclear matter undergoes a deconfinement transition to a new phase of quarks and gluons[1]. Although this has been observed in ultrarelativistic heavy-ion collisions[2,3], it is currently an open question whether quark matter exists inside neutron stars[4]. By combining astrophysical observations and theoretical ab initio calculations in a model-independent way, we find that the inferred properties of matter in the cores of neutron stars with mass corresponding to 1.4 solar masses ($M_\odot$) are compatible with nuclear model calculations. However, the matter in the interior of maximally massive stable neutron stars exhibits characteristics of the deconfined phase, which we interpret as evidence for the presence of quark-matter cores. For the heaviest reliably observed neutron stars[5,6] with mass $M \approx 2M_\odot$, the presence of quark matter is found to be linked to the behaviour of the speed of sound c_s in strongly interacting matter. If the conformal bound $c_s^2 \leq 1/3$ (ref. [7]) is not strongly violated, massive neutron stars are predicted to have sizable quark-matter cores. This finding has important implications for the phenomenology of neutron stars and affects the dynamics of neutron star mergers with at least one sufficiently massive participant.

limit of very high densities, perturbative-QCD (pQCD) techniques, rooted in high-energy particle phenomenology and built on deconfined quark and gluon degrees of freedom[12,13], become accurate, providing the quark-matter EoS to the same accuracy at densities $n \gtrsim 40 n_0 \equiv n_{\mathrm{pQCD}}$.

In the above two limits, QCD matter is known to exhibit markedly different properties. High-density quark matter is approximately scale-invariant, or conformal, whereas in hadronic matter the number of degrees of freedom is much smaller and scale invariance is also violated by the breaking of chiral symmetry. These qualitative differences are reflected in the values taken by different physical quantities. The speed of sound takes the constant value $c_s^2 = 1/3$ in exactly conformal matter and slowly approaches this number from below in high-density quark matter[12]. By contrast, in hadronic matter, the quantity varies considerably: below saturation density, CET calculations indicate $c_s^2 \ll 1/3$, while at higher densities most hadronic models predict $\max(c_s^2) \gtrsim 0.5$. The polytropic index $\gamma \equiv \mathrm{d}(\ln p)/\mathrm{d}(\ln \epsilon)$, on the other hand, has the value $\gamma = 1$ in conformal matter, while both CET calculations and hadronic models generically predict $\gamma \approx 2.5$ around and above saturation density. Finally, the number of degrees of freedom is reflected in the pressure normalized by that of free quark matter (the Fermi-Dirac (FD) limit), p/p_{FD} (ref. [12]). This quantity obtains values of order 0.1 in CET calculations and hadronic models,

E. Annala et al., Nature Physics vol. 16, 907-910 (2020)

At high density (NSs), hadronic matter undergo phase transition to deconfined quark matter forming hybrid stars (HSs).

Basic Mechanism

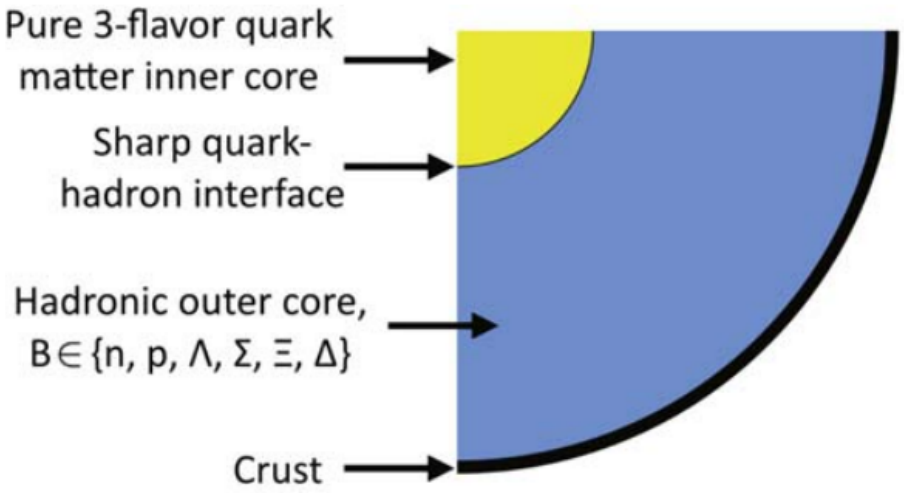

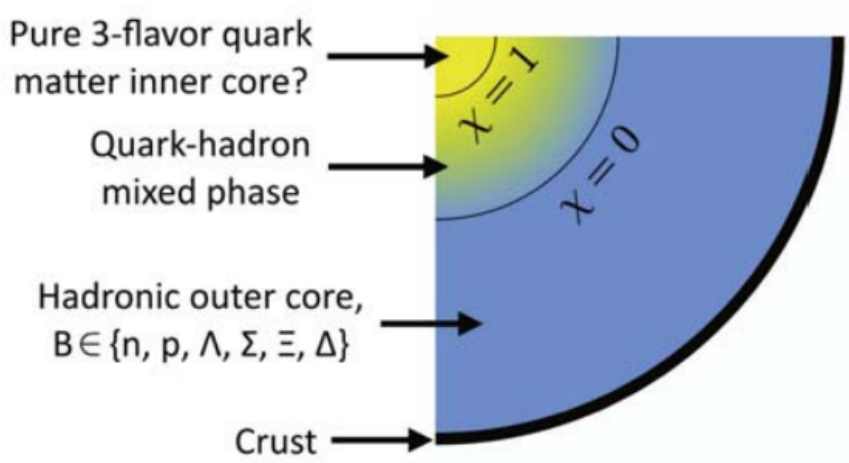

Maxwell construction and Gibbs construction

©M. G. Orsaria et al., J. Phys. G: Nucl. Part. Phys. 46 (2019) 073002

In collaboration with N. Alam and G. Chaudhuri, VECC, Kolkata, India

Pure Hadronic Phase

β equilibrated NSM (n,p,e,μ)

The saturated nuclear matter properties for six RMF hadronic models.

Model	ρ_0 (fm^{-3})	B/A (MeV)	K_0 (MeV)	J_0 (MeV)	L_0 (MeV)
TM1	0.145	−16.26	281.2	36.9	110.8
BSR2	0.149	−16.03	240.0	31.4	62.2
BSR6	0.149	−16.13	235.9	35.4	85.6
GM1	0.153	−16.30	300.1	32.5	93.9
NL3$\omega\rho$4	0.148	−16.25	271.6	33.1	68.2
NL3	0.148	−16.25	271.6	37.4	118.5

Pure Quark Phase

3 flavor SQM (u,d,s,e) with the MIT Bag Model [3]

Quarks constrained within hypothetical region (Bag), characterized by specific bag pressure B that determines the strength of quark interaction.

Density dependent bag pressure

Hadron-quark phase transition at particular density $\rightarrow$ vanishing difference between perturbative and non-perturbative (true) vacuum $\rightarrow$ quarks become asymptotic $\rightarrow$ density dependence of B.
Following a Gaussian distribution [4]

$$B(\rho) = B_{as} + (B_0 - B_{as}) \exp\left[-\beta(\rho/\rho_0)^2\right]$$

where $B_0 = B(\rho = 0)$ and B_{as} - value of $B(\rho)$ where quarks become asymptotic. We choose $B_0 = 400$ MeV fm^{-3} and $\beta = 0.17$ following Burgio et al. We vary B_{as}.

[3] A. Chodos et al., PRD 9, 3471 (1974)
[4] G. F. Burgio et al., PLB526 (2002) 19-26; PRC66 (2002) 025802.

Mechanism of Phase Transition

Maxwell Construction ($\sigma \gtrsim 70$ MeV/fm^2) [5]

Local charge neutrality: $q_H(\mu_B, \mu_e) = 0$

$$q_Q(\mu_B, \mu_e) = 0$$

Maxwell criteria: $P_H(\mu_B, \mu_e) = P_Q(\mu_B, \mu_e)$

$$\mu_B^H = \mu_B^Q$$

$$\mu_e^H \neq \mu_e^Q$$

Jump in density

[5] T. Maruyama et al., PLB 659 (2008) 192

Structure of Neutron Stars

Tolman-Oppenheimer-Volkoff Equations

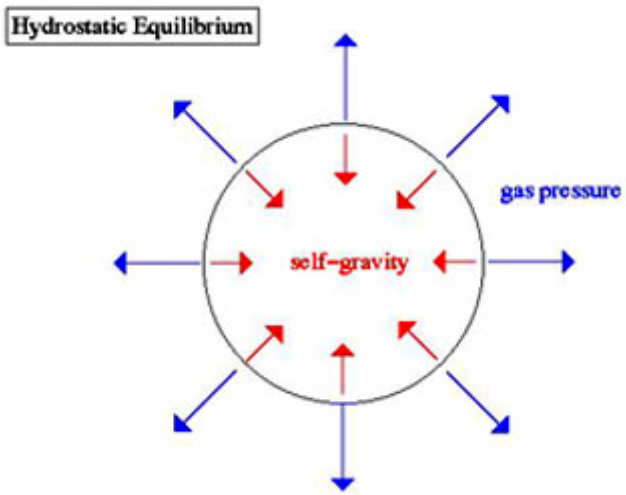

$$\frac{dP}{dr} = -\frac{G}{r}\frac{(\varepsilon + P)\left(M + 4\pi r^3 P\right)}{(r - 2GM)}$$

$$\frac{dM}{dr} = 4\pi r^2 \varepsilon$$

Tidal deformability

$$\Lambda = \frac{2}{3} k_2 (R/M)^5$$

where, k_2 is the tidal Love number

Results

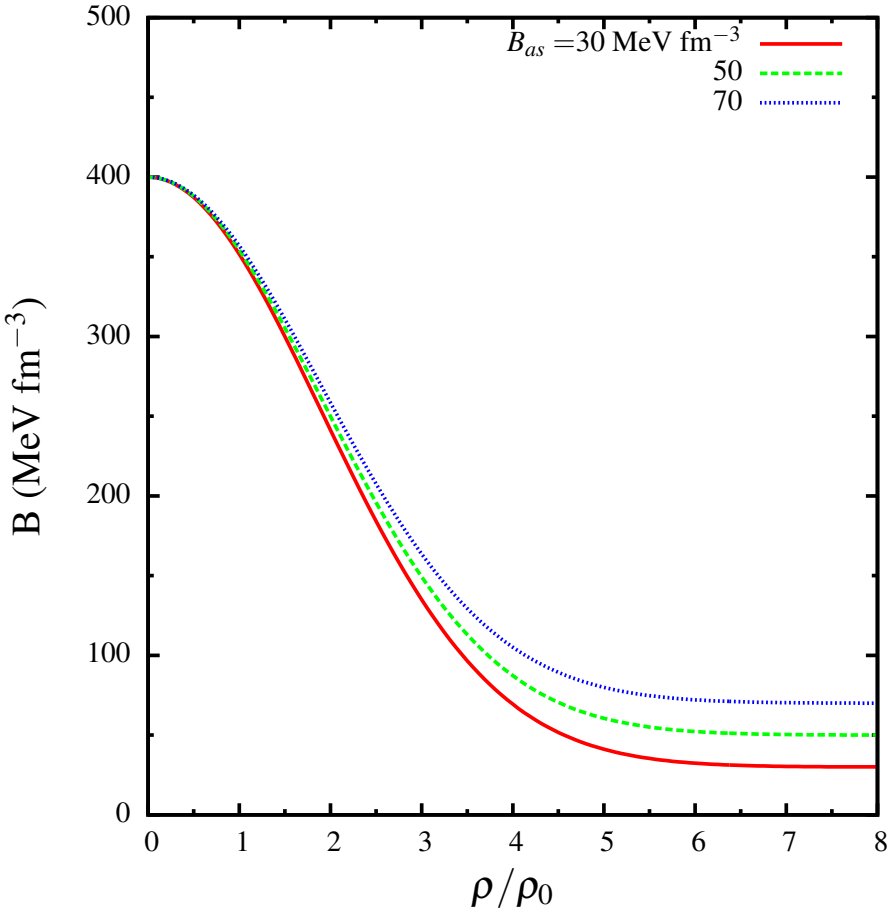

Variation of bag pressure $B(\rho)$ with respect to density for different values of B_{as}.

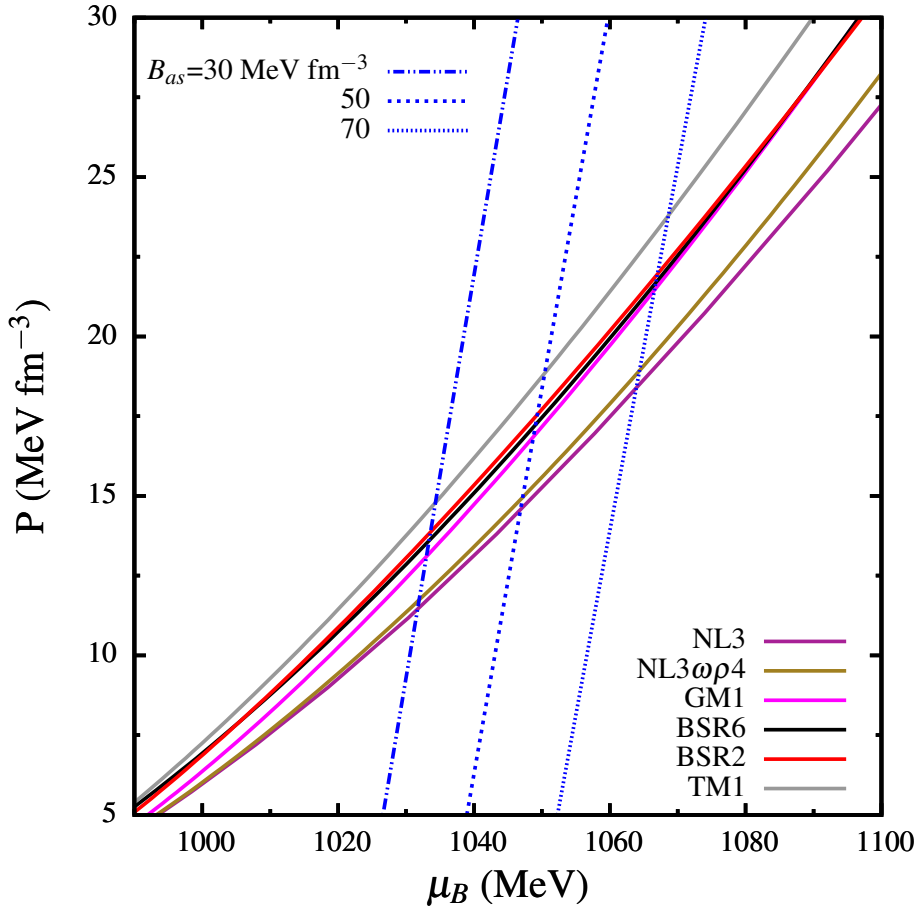

Hadron-quark crossover in the $\mu_B - P$ plane.

DS, N. Alam, and G. Chaudhuri, Phys.Rev D 106, 083008 (2022)

Results

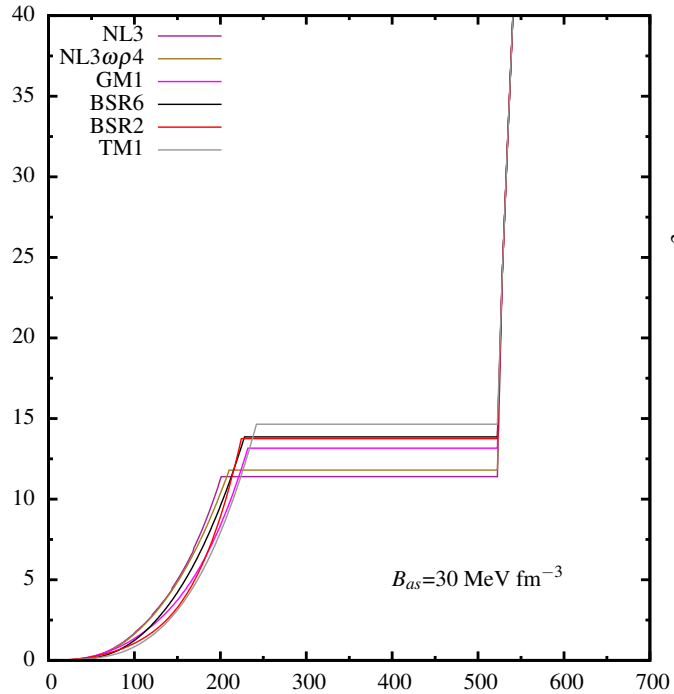

Hybrid EoS with different hadronic models and DDBM with B_{as} =30 MeV fm^{-3}.

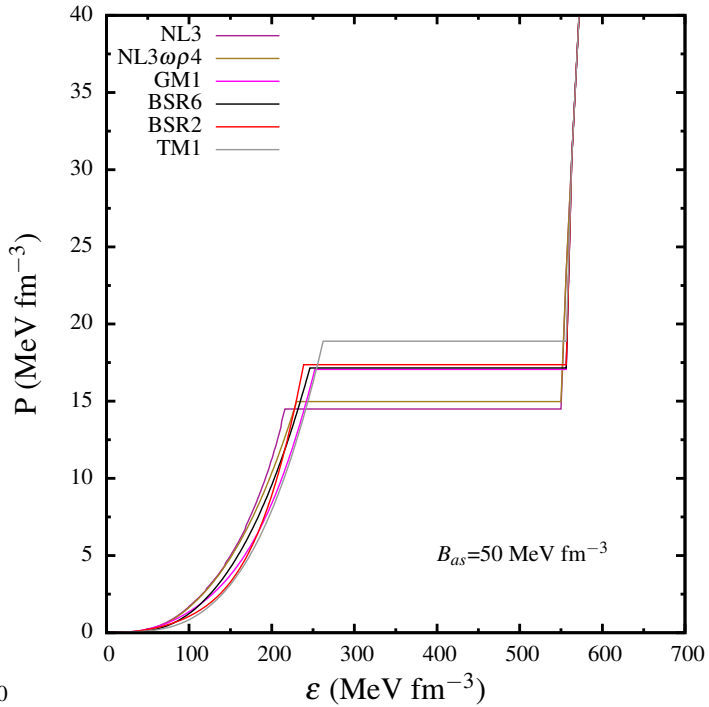

Hybrid EoS with different hadronic models and DDBM with B_{as} =50 MeV fm^{-3}.

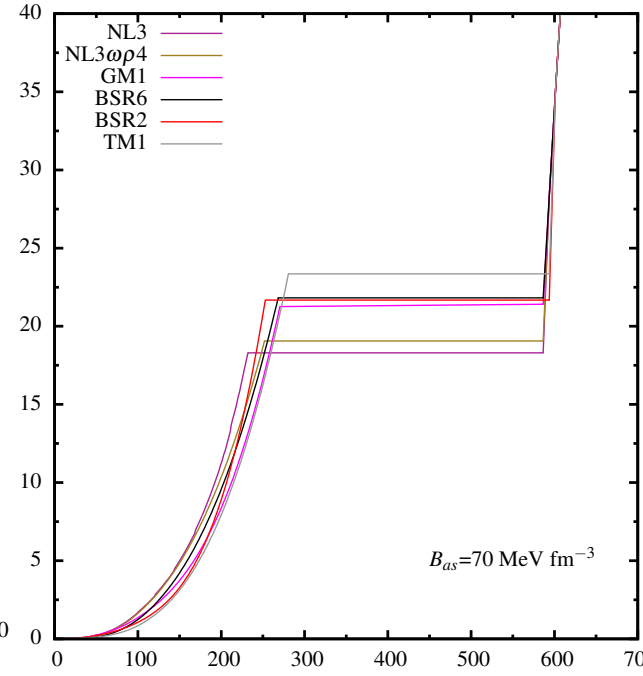

Hybrid EoS with different hadronic models and DDBM with B_{as} =70 MeV fm^{-3}.

DS, N. Alam, and G. Chaudhuri, Phys.Rev D 106, 083008 (2022)

Results

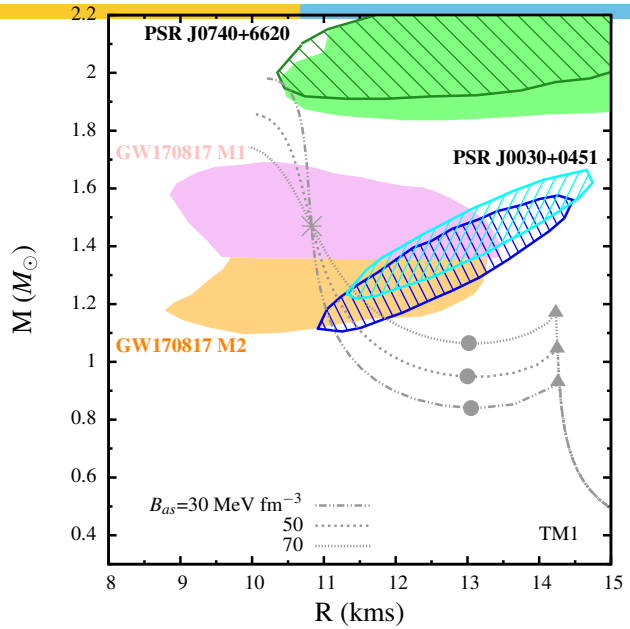

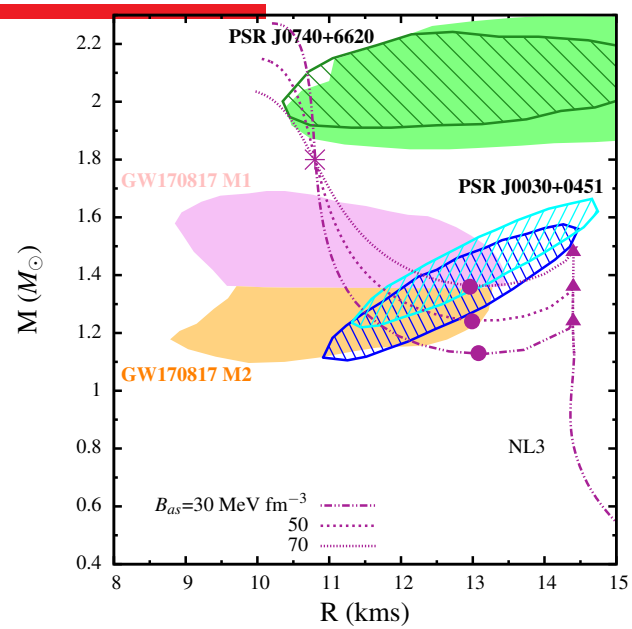

Mass-radius relation of HSs with hadronic models TM1 & NL3 and DDBM with different B_{as}.

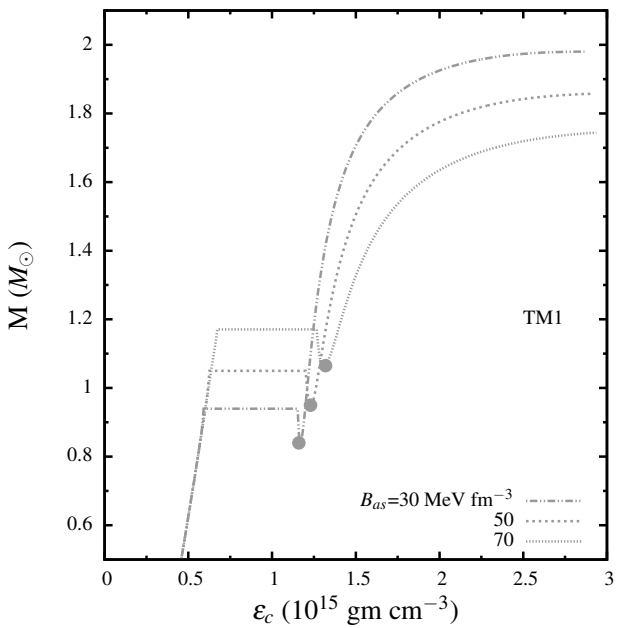

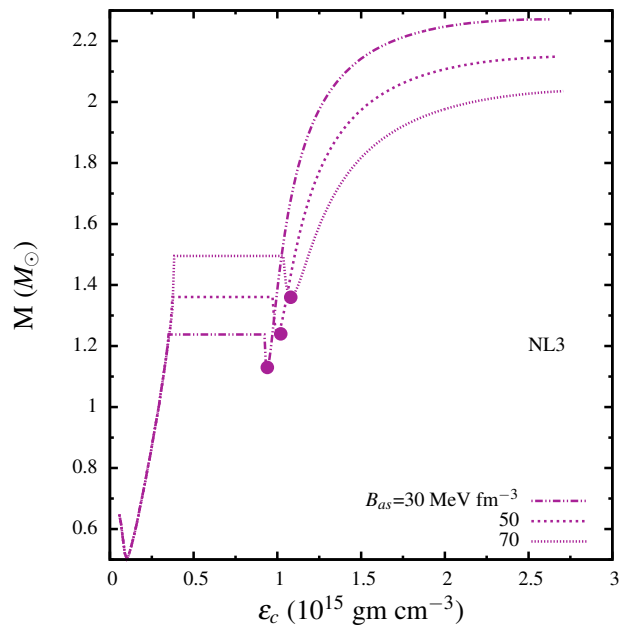

Corresponding central density vs mass relation.

Results

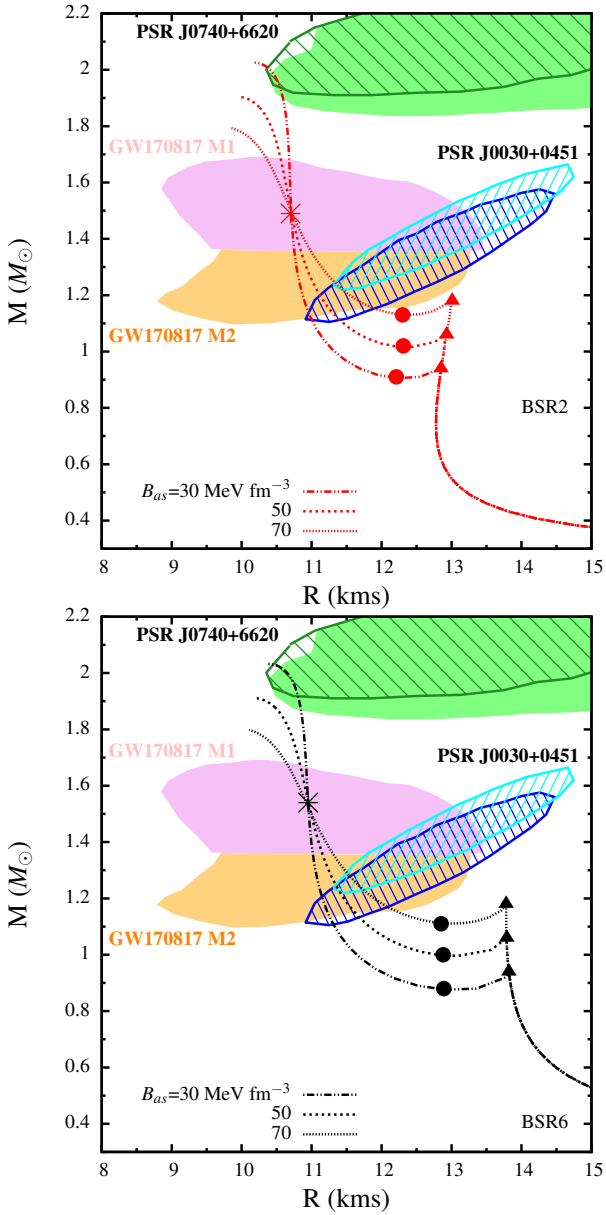

Mass-radius relationship of HSs with hadronic models BSR2 (top) and BSR6 (down) and DDBM with different values of B_{as}.

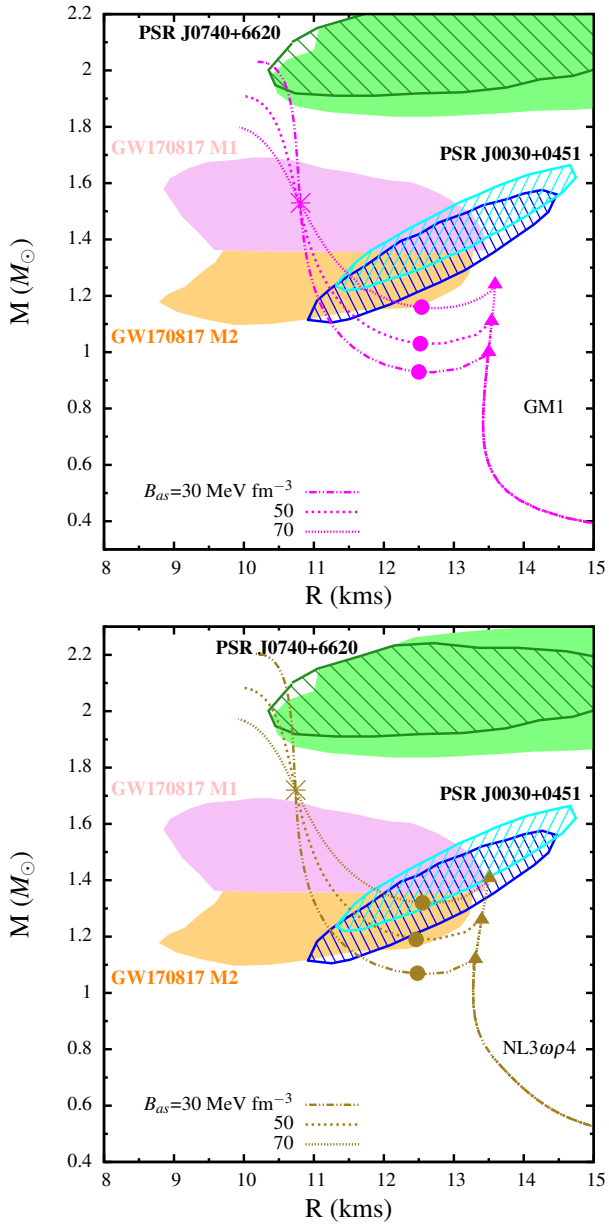

Mass-radius relationship of HSs with hadronic models GM1 (top) and NL3$\omega\rho4$ (down) and DDBM with different values of B_{as}.

Results

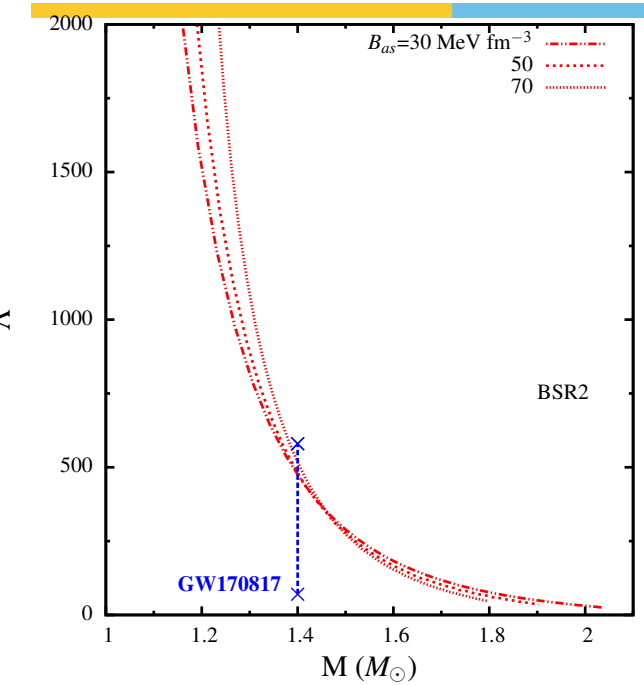
B_{as}=30 MeV fm^{-3}
50
70
BSR2
GW170817
Λ
M ($M_\odot$)

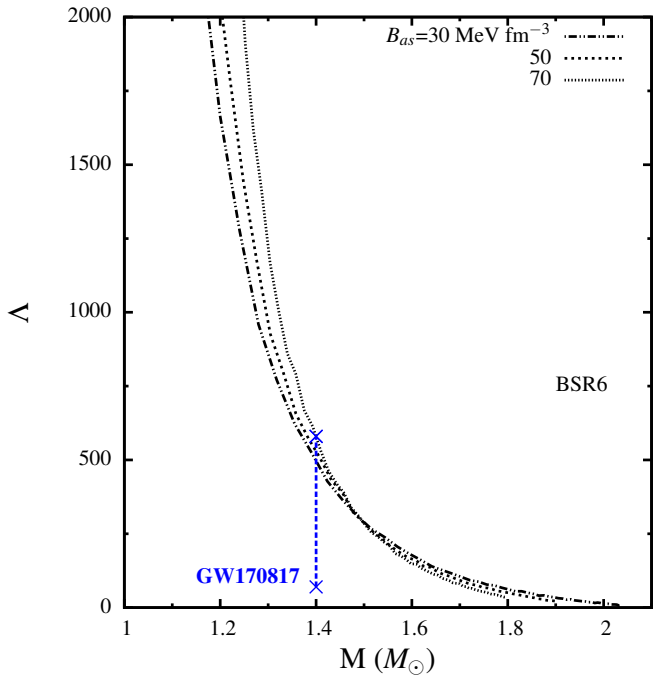
B_{as}=30 MeV fm^{-3}
50
70
BSR6
GW170817
Λ
M ($M_\odot$)

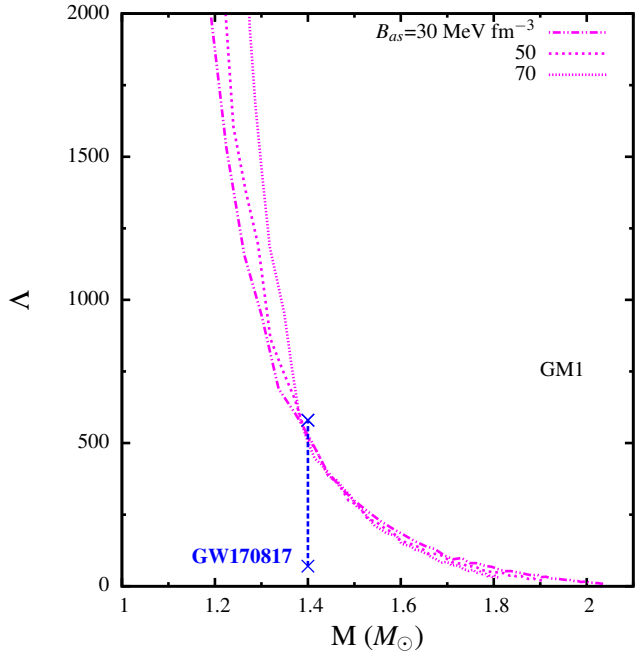
B_{as}=30 MeV fm^{-3}
50
70
GM1
GW170817
Λ
M ($M_\odot$)

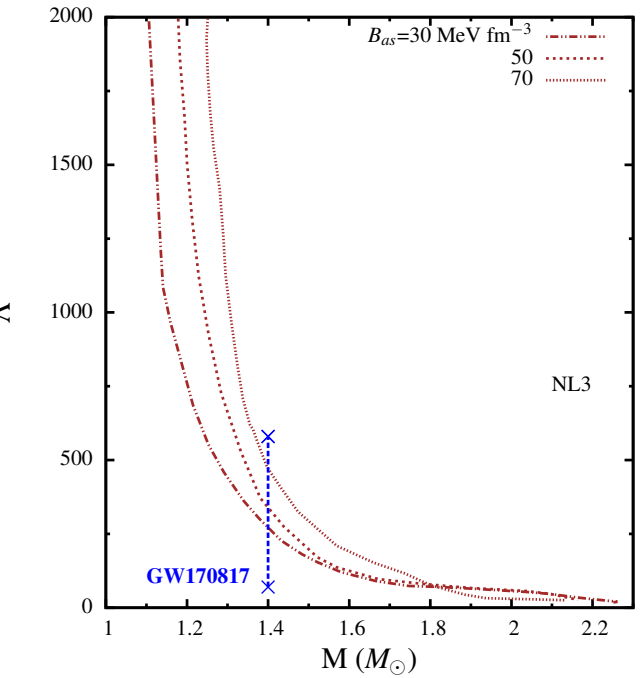
B_{as}=30 MeV fm^{-3}
50
70
NL3
GW170817
Λ
M ($M_\odot$)

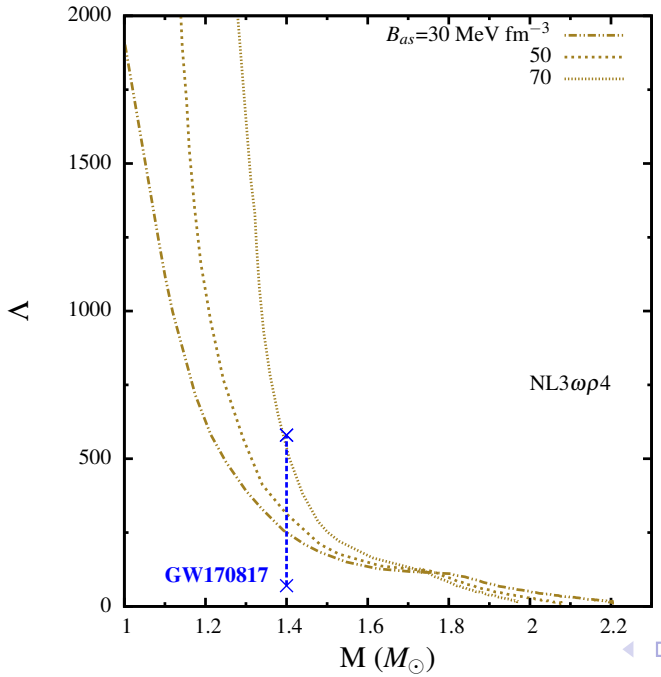
B_{as}=30 MeV fm^{-3}
50
70
NL3$\omega\rho$4
GW170817
Λ
M ($M_\odot$)

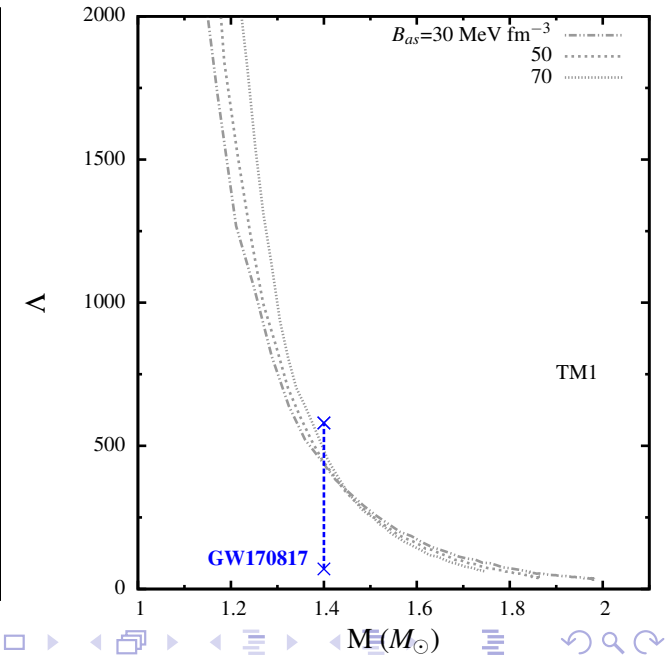
B_{as}=30 MeV fm^{-3}
50
70
TM1
GW170817
Λ
M ($M_\odot$)

Results

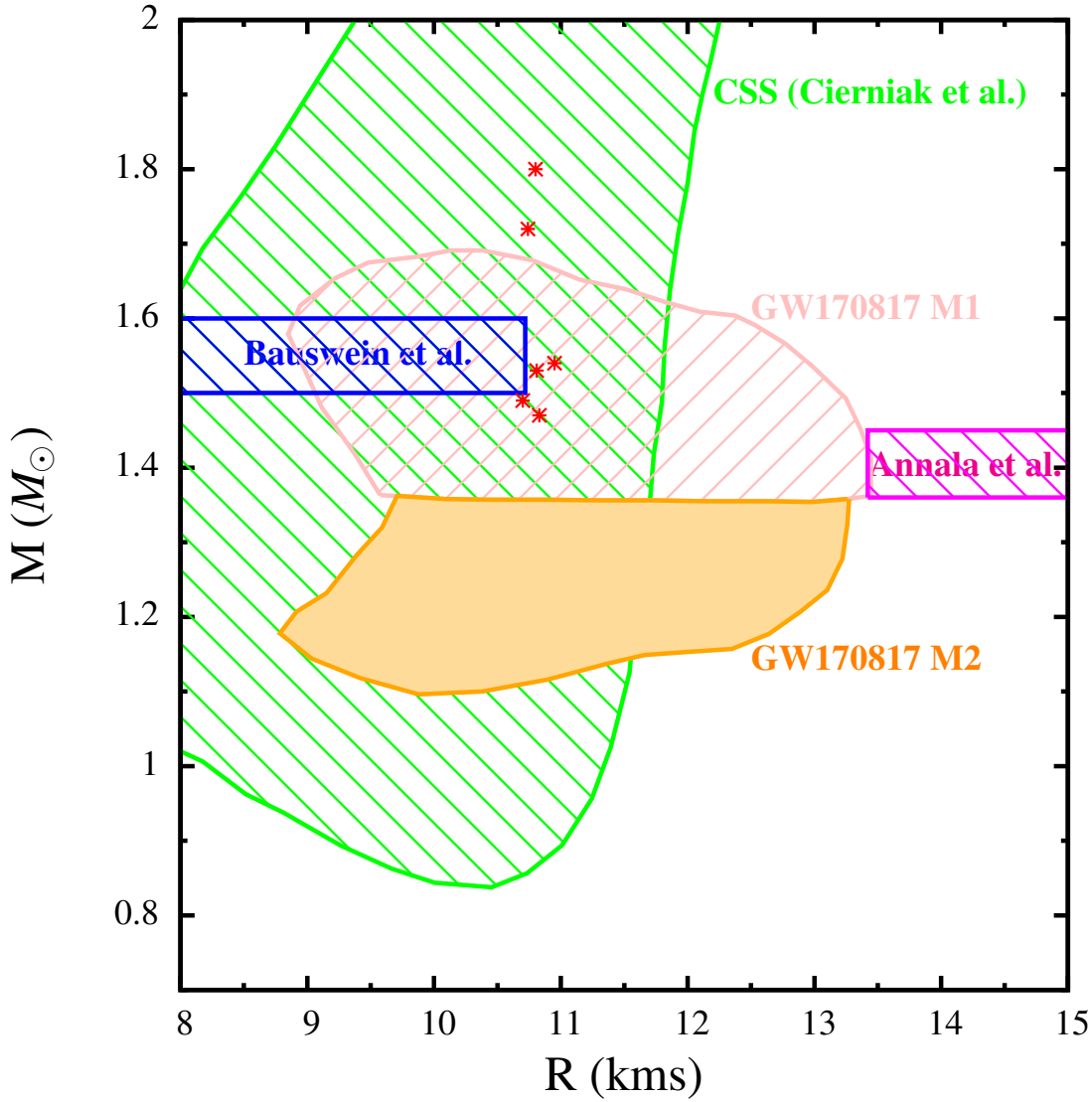

Location of special points on the mass-radius plot of hybrid stars with different hadronic models.

Results

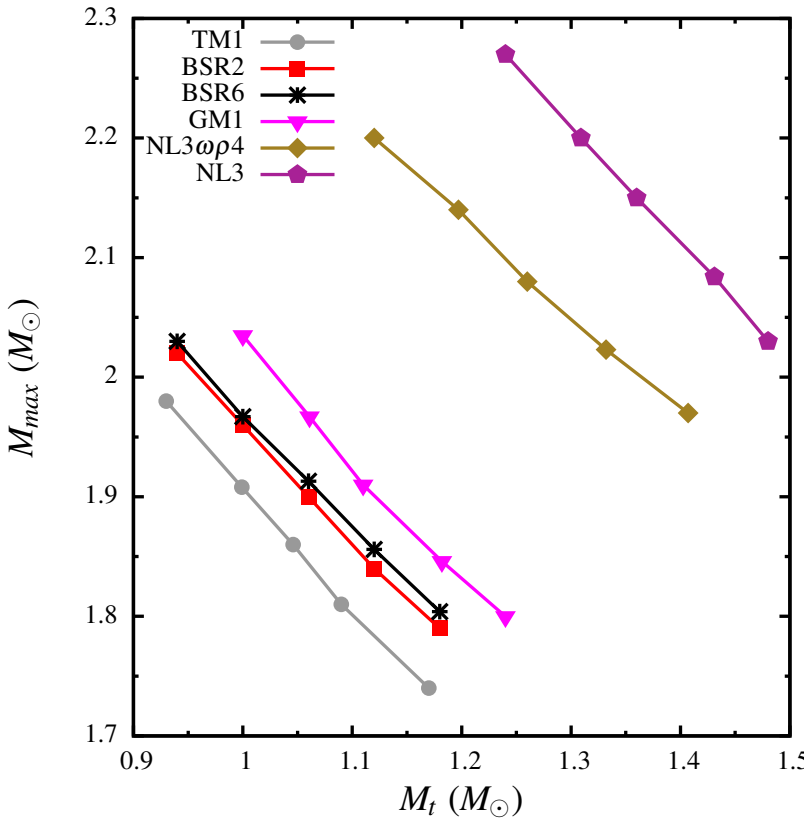

Variation of maximum mass (M_{max}) with respect to transition mass (M_t) of the HSs with different hadronic models. The points represent different the values of M_{max} and M_t for different values of B_{as}.

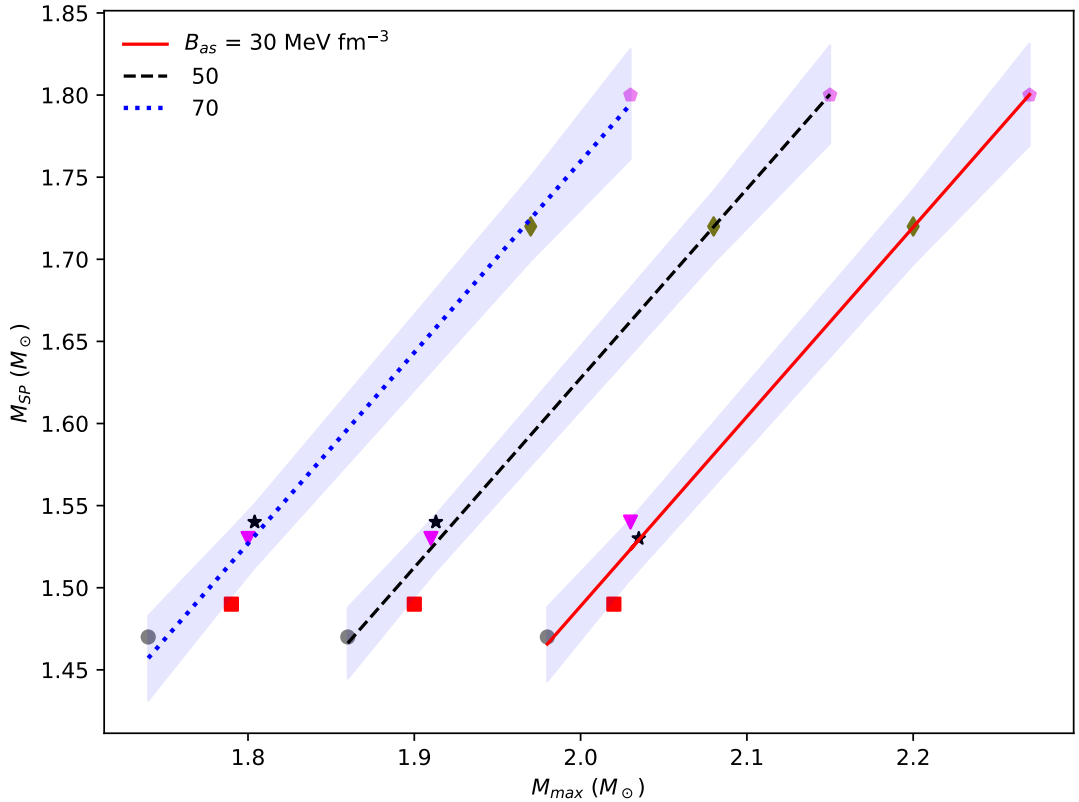

Variation of mass corresponding to special point (M_{SP}) with respect to maximum mass (M_{max}) of a HSs with different hadronic models. The different lines represent the fitted functions for different values of B_{as}.

Universal Relations: $M_{SP} = -C_1 + C_2 M_{max}$

where C_1 and C_2 are constants whose values depend on B_{as}

DS, N. Alam, and G. Chaudhuri, Phys.Rev D 106, 083008 (2022)

Summary and Conclusions

- Hadron-quark phase transition in neutron star cores is achieved in the present work with the help of Maxwell construction.
- For the purpose we employ six different and well-known RMF models for the pure hadronic phase. The quark phase is described with the MIT Bag model in which the density dependence of the bag pressure is invoked for different asymptotic values of the bag pressure via a Gaussian relation.
- For the variation of B_{as}, the calculated HS properties satisfy the present day astrophysical constraints on the structural properties of compact stars.
- The resulting HS configurations exhibit twin star characteristics and distinct SPs on the mass-radius diagram, irrespective of the transition densities and the value of B_{as}.
- The location of the SPs for different hadronic models do not depend on the transition density. For any particular value of B_{as}, the mass corresponding to SP (M_{SP}) and the maximum mass (M_{max}) of the HSs, follow a nearly linear (fitted) relationship, where the slope is independent of the value of B_{as} - universal relations in the context of formation of SPs.

Modified Bag Model with Repulsive Interaction

$$\Omega_f = -\frac{\gamma_f}{24\pi^2}\left[\mu_f\sqrt{\mu_f^2-m_f^2}\left(\mu_f^2-\frac{5}{2}m_f^2\right)+\frac{3}{2}m_f^4\,ln\left(\frac{\mu_f+\sqrt{\mu_f^2-m_f^2}}{m_f}\right)\right.$$

$$\left.-\frac{2\alpha}{\pi}\left\{3\left(\mu_f\sqrt{\mu_f^2-m_f^2}-m_f^2\,ln\frac{\mu_f+\sqrt{\mu_f^2-m_f^2}}{m_f}\right)^2-2\left(\mu_f^2-m_f^2\right)^2-3m_f^4\,ln^2\left(\frac{m_f}{\mu_f}\right)\right\}\right]$$

$$\Omega = \Omega_f + \Omega_e + B$$

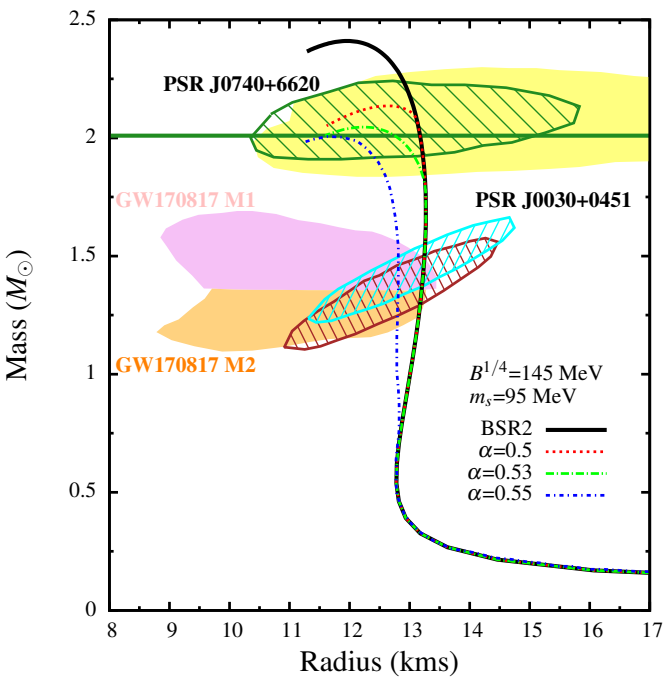

Mass-radius relation of HSs for different values of repulsive interaction coupling parameter α

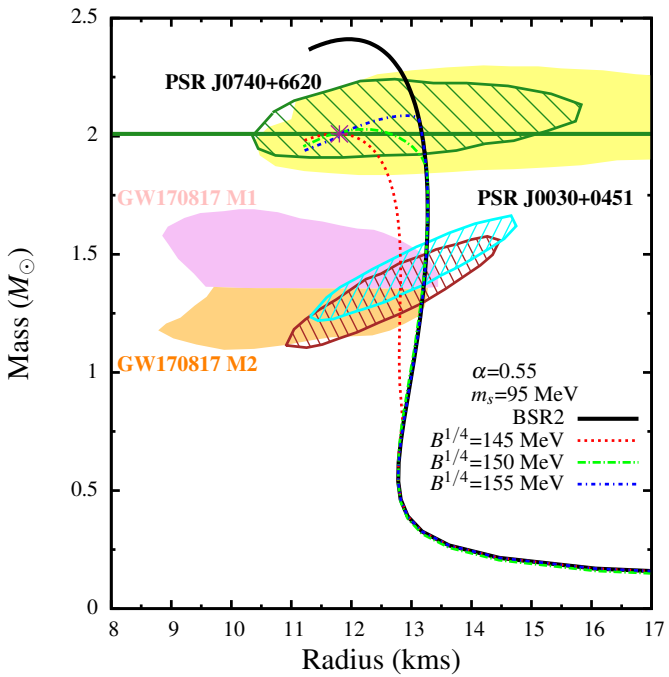

Mass-radius relation of HSs for different values of bag constant B.

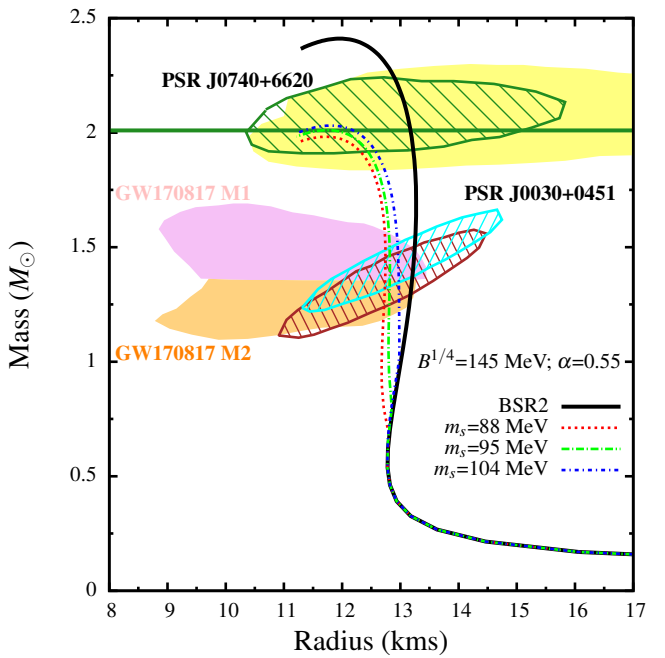

Mass-radius relation of HSs for different values of s quark mass m_s.

S. Pal, S. Podder, DS, and G. Chaudhuri, Phys.Rev.D 107 (2023) 6, 063019

Vector Bag (vBag) Model

$$\mathcal{L} = \sum_f \left[\overline{\psi}_f \left\{ \gamma^\mu (i\partial_\mu - g_{qqV} V_\mu) - m_f \right\} \psi_f - B \right] \Theta(\overline{\psi}_f \psi_f)$$

$$+ \frac{1}{2} m_V^2 V_\mu V^\mu - \frac{1}{4} V_{\mu\nu} V^{\mu\nu} + b_4 \frac{(g^2 V_\mu V^\mu)^2}{4} + \overline{\psi}_l (i\gamma_\mu \partial^\mu - m_l) \psi_l$$

$$X_V = g_{ssV}/g_{uuV} \text{ and } G_V = (g_{uuV}/m_V)^2$$

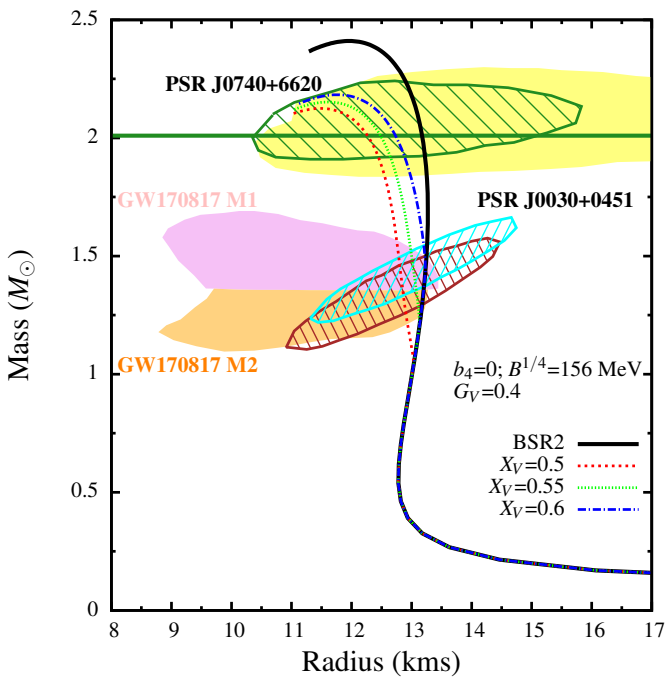

Mass-radius relation of HSs for different values of X_V

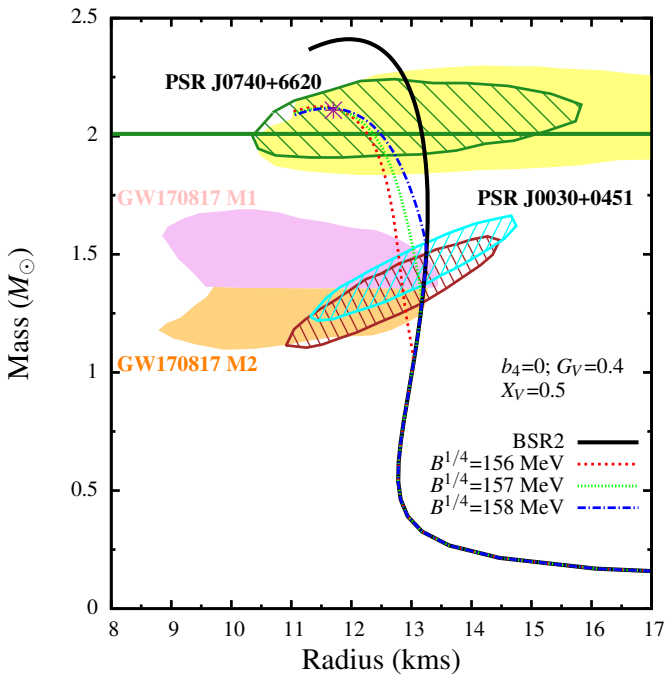

Mass-radius relation of HSs for different values of bag constant B.

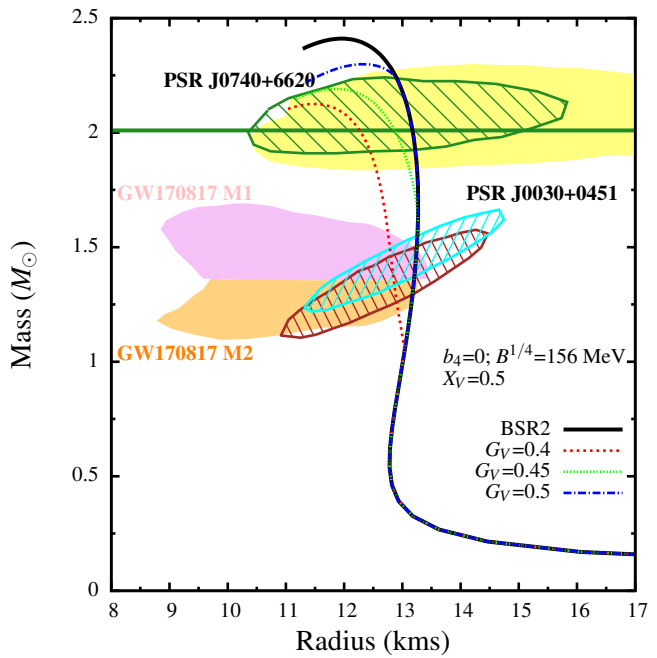

Mass-radius relation of HSs for different values of G_V.

S. Pal, S. Podder, DS, and G. Chaudhuri, Phys.Rev.D 107 (2023) 6, 063019

Density Dependent Bag Model with Gaussian Form

$$B(\rho) = B_{as} + (B_0 - B_{as}) \exp\left[-\beta(\rho/\rho_0)^2\right]$$

$$\Delta B = B_0 - B_{as}$$

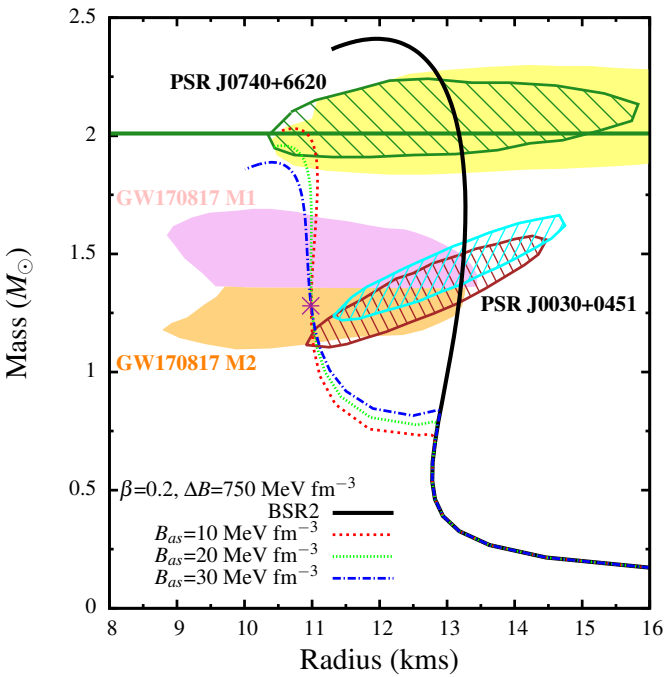

Mass-radius relation of HSs for different values of B_{as}

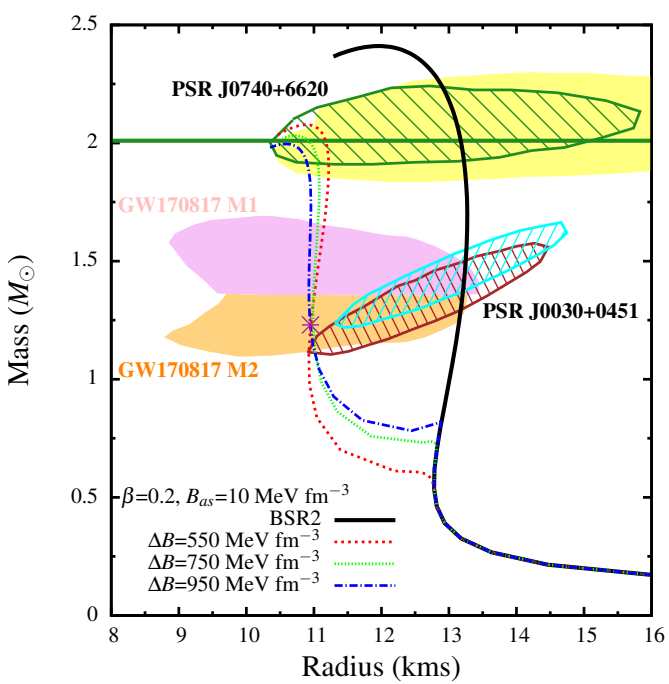

Mass-radius relation of HSs for different values of bag constant ΔB.

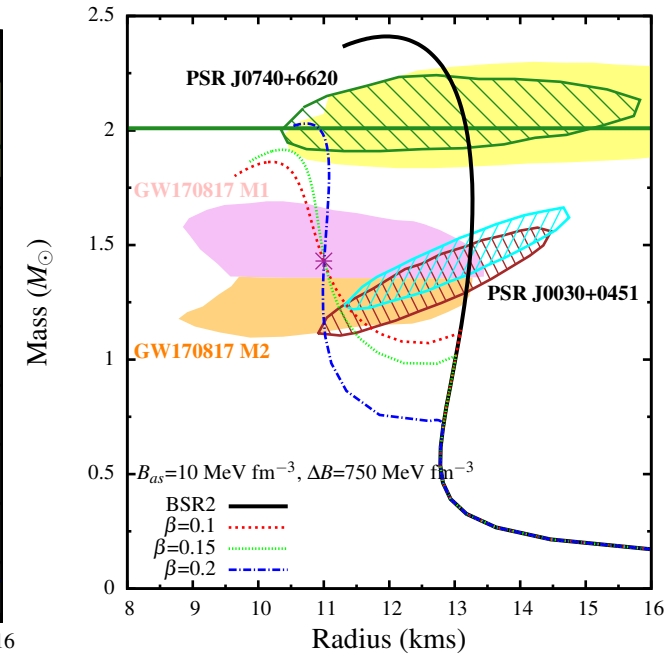

Mass-radius relation of HSs for different values of β.

S. Pal, S. Podder, DS, and G. Chaudhuri, Phys.Rev.D 107 (2023) 6, 063019

Density Dependent Bag Model with Hyperbolic Form

$$B(\rho) = B_0 * f(\rho)$$

$$f(\rho) = \frac{1}{2}\left[1 - tanh\left(\frac{\rho - \bar{\rho}}{\Gamma_\rho}\right)\right]$$

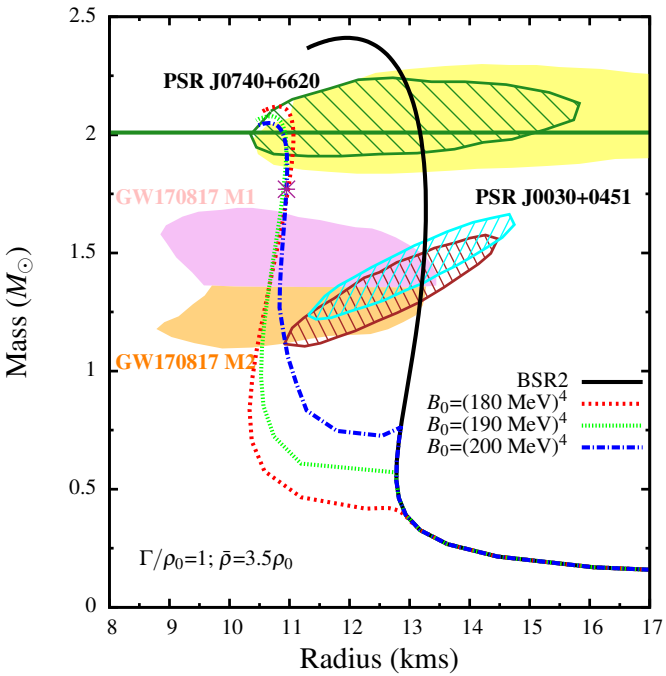

Mass-radius relation of HSs for different values of $B0$

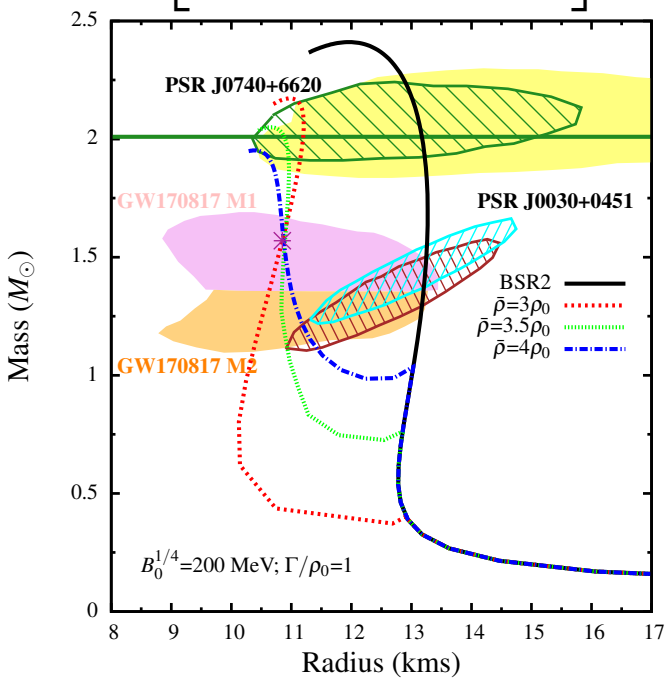

Mass-radius relation of HSs for different values of bag constant $\bar{\rho}$.

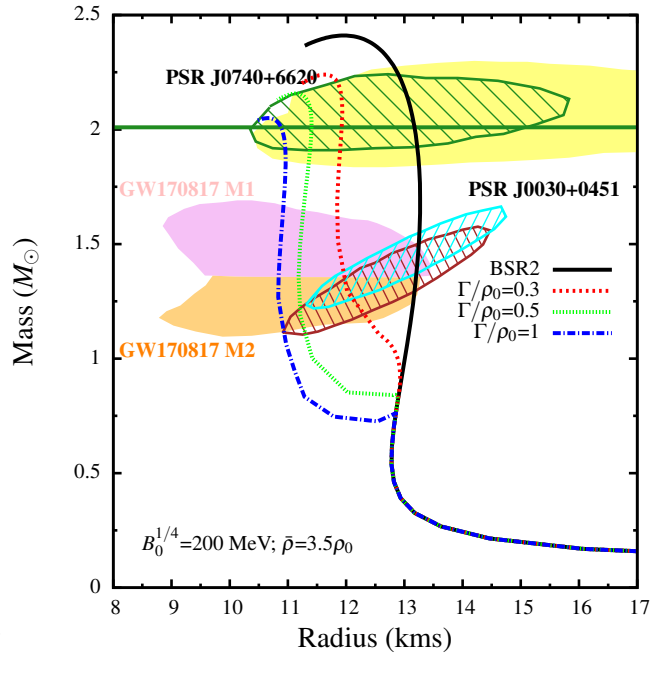

Mass-radius relation of HSs for different values of Γ/ρ_0.

S. Pal, S. Podder, DS, and G. Chaudhuri, Phys.Rev.D 107 (2023) 6, 063019

Phase transition with BSR2 hadronic model & different quark models

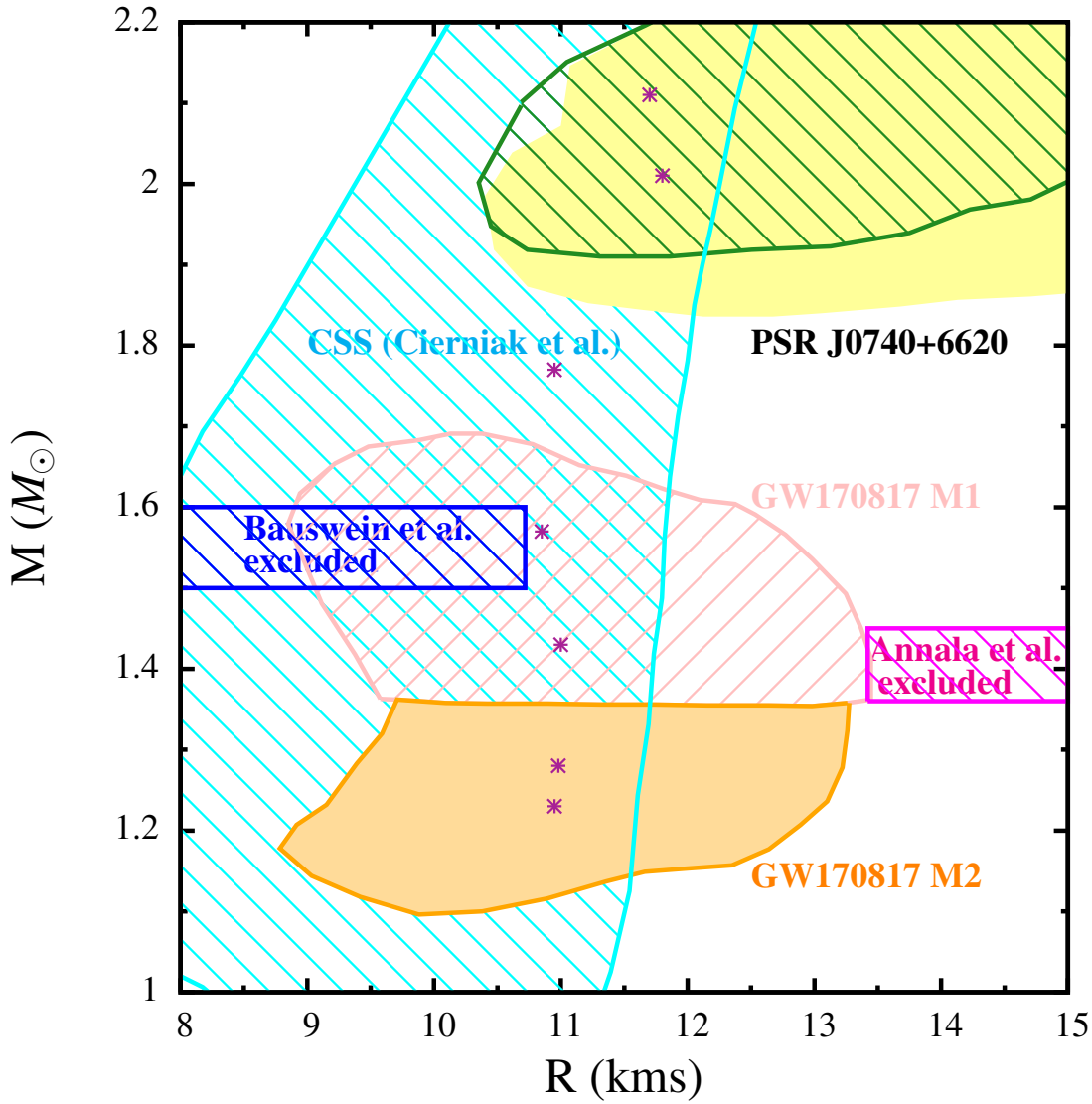

Location of special points on the mass-radius plot of hybrid stars with different quark models.

Summary and Conclusions

- Hadron-quark phase transition in neutron star cores is achieved in the present work with the help of Maxwell construction.
- We choose a fixed relativistic mean-field hadronic model BSR2 and four different forms of MIT bag model for the quark phase (two forms with DIBP and two forms with DDBP).
- For each quark model, we varied one parameter at a time keeping the others fixed and calculated the HS properties.
- The HS configurations obtained with all the four quark models can satisfy the present day astrophysical constraints on the structural properties of compact stars.
- Twin star characteristics is obtained in certain cases only when the bag pressure is considered to be density dependent and not when it is taken to be constant.
- The bag pressure plays immense role in the emergence of SPs in both density dependent and independent scenarios.
- No other parameter associated with the four quark models can lead to the formation of SPs.

References

- A. V. Yudin et al., Astronomy Letters, 40, 2014, 201.
- M. Cierniak and D. Blaschke, Eur. Phys. J. Spec. Top. 229, 3663-3673 (2020).
- A. Ayriyan, D. Blaschke, A. G. Grunfeld, D. Alvarez-Castillo, H. Grigorian, and V. Abgaryan, Eur. Phys. J. A57, 318 (2021); Phys. Rev. C 97, 045802 (2018).
- A. Ayriyan, D. Blaschke, A. G. Grunfeld, D. Alvarez-Castillo, H. Grigorian, and V. Abgaryan, Phys. Rev. C 97, 045802 (2018).
- G. Montana, L. Tolos, M. Hanauske, and L. Rezzolla, Phys. Rev. D 99, 103009 (2019).
- J.-E. Christian and J. Schaffner-Bielich, Astrophys. J. Lett. 894, L8 (2020).
- Z. Sharifi, M. Bigdeli, and D. Alvarez-Castillo, Phys. Rev. D 103, 103011 (2021).


thank
you